2013

Structure and magnetism of dilute Co(Zr) nanoclusters

Bhaskar Das
University of Nebraska-Lincoln, bhaskar.das@huskers.unl.edu

Balamurugan Balamurugan
University of Nebraska-Lincoln, balamurugan@unl.edu

Ralph Skomski
University of Nebraska at Lincoln, rskomski2@unl.edu

Xingzhong Li
University of Nebraska-Lincoln, xli2@unl.edu

Pinaki Mukherjee
University of Nebraska-Lincoln, pinaki.mukherjee@rutgers.edu

See next page for additional authors

Structure and magnetism of dilute Co(Zr) nanoclusters

B. Das,[1,2,a)] B. Balamurugan,[1,2] R. Skomski,[1,2] X. Z. Li,[1] P. Mukherjee,[1,3] G. C. Hadjipanayis,[4] and D. J. Sellmyer[1,2]
[1]*Nebraska Center for Materials and Nanoscience, University of Nebraska, Lincoln, Nebraska 68588, USA*
[2]*Department of Physics and Astronomy, University of Nebraska, Lincoln, Nebraska 68588, USA*
[3]*Department of Mechanical and Materials Engineering, University of Nebraska, Lincoln, Nebraska 68588, USA*
[4]*Department of Physics and Astronomy, University of Delaware, Newark, Delaware 19716, USA*

(Presented 18 January 2013; received 31 October 2012; accepted 3 December 2012; published online 18 March 2013)

Co(Zr) nanoclusters having a small fraction of Zr ($\leq$7.8 at. %) were produced using a cluster-deposition method and aligned using a magnetic field of about 5 kOe prior to deposition. This study shows that Zr addition to Co nanoclusters improves the fraction of hexagonal close-packed structure, magnetic anisotropy, and easy-axis alignment process. Co(Zr) nanoclusters having 7.8 at. % of Zr exhibit a considerably enhanced magnetic anisotropy constant $K_1 \approx 6.7$ Mergs/cm^3 and coercivity $H_c \approx 700$ Oe at 300 K as compared to those of Co nanoclusters ($K_1 \approx 2.9$ Mergs/cm^3 and $H_c \approx 180$ Oe). © *2013 American Institute of Physics*. [http://dx.doi.org/10.1063/1.4795318]

Research on specially designed magnetic nanoparticles provides new insights into nanoscale phenomena and also may lead to new materials for additional technological requirements.[1–3] Recently, simple ferromagnetic nanoparticles such as Fe or Co doped with substitutional or interstitial additives have gained significant attention in order to create nanoparticle building-blocks with improved magnetic anisotropies for alternative permanent-magnet materials. They are also of interest from the viewpoint of fundamental understanding of nanoscale effect on electronic structure and magnetism.[4–6] It is worth noting that experimental and theoretical investigations on bulk and thin films of Fe and Co already have shown appreciable changes in magnetic properties on doping with various transition metals.[7–9]

The fabrication of nanoparticles, however, requires sophisticated methods that ideally have precise control over the size, size-distribution, crystal structure, and composition. In this regard, the gas-aggregation-type cluster-deposition method has been shown to produce assemblies of magnetic nanoclusters smaller than 15 nm with a narrow size distribution and having standard or new crystal structures and stoichiometries.[10–16] Most importantly, the easy axes also can be aligned by applying a magnetic field to the nanoclusters before deposition and this is an important processing step for implementing nanoclusters in practical applications.[10] In the present study, we have used a cluster-deposition system to produce dilute ($Co_{1-x}Zr_x$) nanoclusters having different at. % of Zr ($0 \leq x \leq 7.8$) and investigated their structural and magnetic properties.

The experimental set up has a water-cooled gas-aggregation chamber,[10] where a composite target of Co-Zr is sputtered by a direct current (DC) magnetron sputtering using a mixture of argon and helium gases to form Co(Zr) nanoclusters. These nanoclusters were extracted as a collimated beam travelling towards the deposition chamber and deposited on a single crystalline Si (001) substrate kept at room temperature. X-ray diffraction (XRD, Rigaku D/Max-B diffractometer), superconducting quantum interference device (SQUID) magnetometer, and energy dispersive x-ray analysis (EDX, JEOL JSM 840A scanning electron microscope) were used to characterize the nanoclusters. For high-resolution transmission-electron microscopy (HRTEM, FEI Tecnai Osiris (Scanning) Transmission Electron Microscope) studies, carbon-coated copper grids were used as substrates for deposition.

XRD patterns of nanoclusters of Co and Co(Zr) having 6.3 at. % of Zr are shown in Fig. 1(a). The standard positions and relative intensities of XRD peaks corresponding to the hexagonal close-packed (hcp) and face-centered cubic (fcc) structures of Co are given as vertical-solid and -dotted lines, respectively.[17,18] XRD pattern of Co nanoclusters shows the most intense diffraction peak close to (002) reflection of the hcp Co, but the presence of a low-intensity (200) reflection also reveals a minor fraction of fcc phase. In the case of Co(Zr) clusters, the (200) reflection of the fcc phase completely disappears and the position of the most intense XRD peak has a good agreement with that of the (002) reflection of the hcp phase as shown in the XRD pattern of Co(Zr) nanoclusters having 6.3 at. % of Zr. These results indicate that Co(Zr) do not have a detectable amount of fcc phase by XRD, revealing predominant hcp structure According to the equilibrium Co-Zr binary phase diagram, $Co_{100-x}Zr_x$ solid solution forms up to 0.2 at. % of Zr.[19] In the present study, non-equilibrium cluster-deposition method produces $Co_{100-x}Zr_x$ nanoclusters for $0 < x \leq 7.8$ and this presumably leads to the stabilization of hcp structure in Co(Zr) nanoclusters. TEM studies show that Co(Zr) nanoclusters have an average size (d) of about 8.0 nm with an rms standard deviation of $\sigma/d = 0.16$ (not shown here). In comparison, Co nanoclusters have a slightly larger average size of about 10 nm. In addition, the HRTEM image of the Co(Zr) nanoclusters indicates a high degree of atomic ordering (Fig. 1(b)), and the corresponding

a)Author to whom correspondence should be addressed. Electronic mail: bhaskar.das@huskers.unl.edu

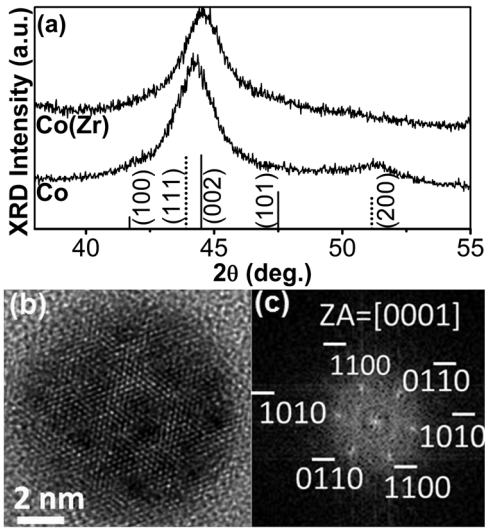

FIG. 1. (a) X-ray diffraction patterns for nanoclusters of Co and Co(Zr) having 6.3 at. % of Zr. The standard positions and relative intensities of XRD peaks corresponding to the hcp and fcc structures of Co are given as vertical-solid and -dotted lines, respectively (b) High-resolution TEM image of Co(Zr) nanoclusters and (c) the corresponding fast Fourier transform along [0001] zonal axis revealing hcp structure.

fast Fourier transform (FFT) image as shown in Fig. 1(c) reveals hcp structure in agreement with the XRD results.

The advantage of the cluster-deposition method is that growth and crystallization of nanoclusters occur directly during the gas-aggregation process, and thus it is possible to align the easy axes by applying a magnetic field using a set of permanent magnets before deposition, as shown in Fig. 2(a).[10] Co and Co(Zr) nanoclusters were aligned using a magnetic field of 5 kOe along the x-axis with respect to substrate as schematically shown in Fig. 2(b). Magnetic properties of aligned nanoclusters were investigated by measuring the magnetization M at 300 K as a function of applied magnetic field H from −70 to 70 kOe along the easy (x-axis) and hard (y-and z-axes) directions. The room-temperature M-H curve of the Co nanoclusters measured along the easy (x-axis) and hard (z-axis) directions are nearly identical with coercivities $H_c \approx 180$ Oe and remanence ratios $M_r/M_s \approx 0.40$ as shown in Fig. 2(c) revealing a poor alignment, where M_s and M_r are saturation and remanent magnetizations, respectively.

In comparison, Co(Zr) nanoclusters having 6.3 at. % of Zr exhibit $H_c \approx 400$ Oe and $M_r/M_s \approx 0.85$ along the easy direction (x-axis) and comparatively reduced $H_c \approx 130$ Oe and $M_r/M_s \approx 0.16$ along the hard direction (z-axis). Note that M-H loop measured along the y-axis for the Co(Zr) nanoclusters is identical to that measured along the z-axis. These results show an effective alignment in Co(Zr) nanoclusters by applying a magnetic field prior to deposition.

As compared to aligned nanoclusters, M-H curves of the unaligned Co and Co(Zr) clusters deposited in the absence of a magnetic field show identical hysteresis loops with M_r/M_s in the range of about 0.40–0.49, suggesting a random distribution of easy axes (not shown here). Note that M_r/M_s is 0.5 for non-interacting randomly oriented nanoclusters. In the present study, Co and Co(Zr) nanoclusters are not embedded in a matrix, and thus some dipolar and exchange interactions are expected between the nanoclusters. The unaligned Co

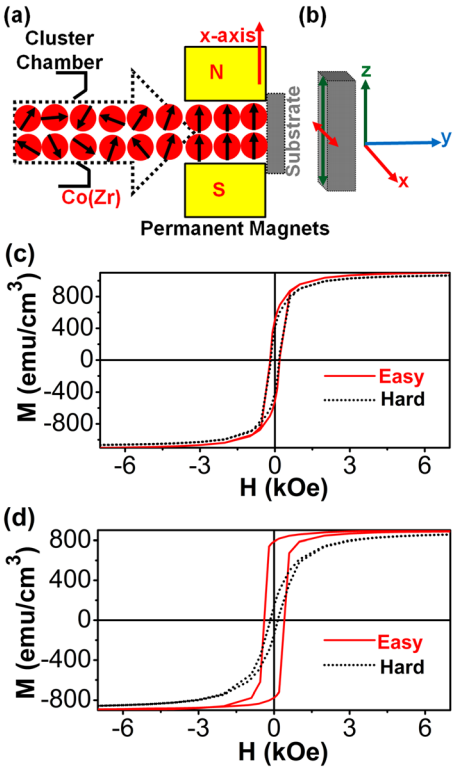

FIG. 2. Easy-axis alignment of Co(Zr) nanoclusters: (a) Schematic illustration of the alignment method using a set of permanent magnets (N-S), prior to deposition on substrate.[10] (b) Three dimensional view of the substrate is also given—in order to show the direction of the applied magnetic field (x-axis) with respect to the substrate plane. The expanded room-temperature M-H curves of the aligned nanoclusters measured along the easy (x-axis) and hard (y-axis) directions: (c) Co and (d) Co(Zr) having 6.3 at. % of Zr.

and Co(Zr) nanoclusters, however, exhibit only slightly less M_r/M_s (about 0.40–0.49) indicating relatively weak or competing exchange and dipolar interactions. In addition, the magnetic anisotropy constant K_1 was estimated by fitting the high field region of M-H curves of unaligned Co and Co(Zr) nanoclusters using the law-of-approach-to-saturation method, widely used for randomly oriented magnets.[20–22] This analysis shows significantly enhanced magnetic anisotropies of Co nanoclusters on Zr addition. For example, the estimated values of K_1 for the nanoclusters of Co and Co(Zr) having 7.8 at. % of Zr are 2.8 and 6.7 Mergs/cm^3, respectively. We also have estimated the magnetic anisotropy constant K_1 for aligned Co(Zr) nanoclusters using the area under the complete M-H curves (from 0 to 70 kOe) along the easy and hard directions.[23] For example, this analysis yield K_1 value of 6.9 Mergs/cm^3 for Co(Zr) nanoclusters having 7.8 at. % of Zr, which is in agreement with those estimated from the law-of-approach-to-saturation method. Note that generally nanoclusters show lower K_1 as compared to standard bulk values, presumably due to disorder and surface effects in nanoclusters.[24] In addition to the increase in anisotropy, Co(Zr) nanoclusters also show appreciable magnetic polarization J_s ($J_s = 4\pi M_s$) in the range of 14.3–10.7 kG on varying Zr content from 2.6 to 7.8 at. %.

The measured values of H_c and M_r/M_s of aligned Co(Zr) nanoclusters as a function of Zr at. % along the easy and hard directions are shown in Figs. 3(a) and 3(b), respectively.

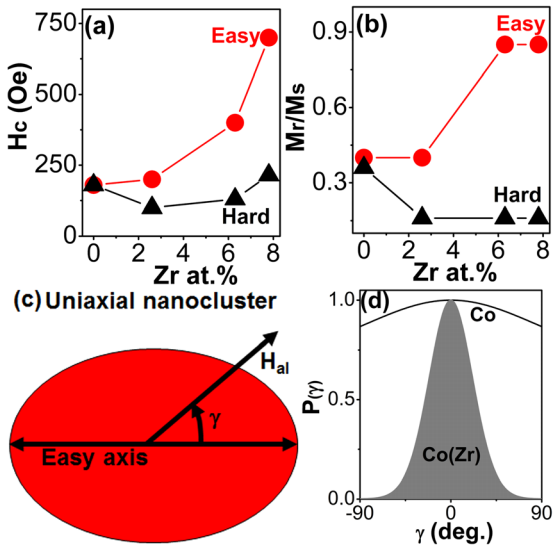

FIG. 3. (a) H_c and (b) M_r/M_s at 300 K of Co(Zr) nanoclusters as a function Zr contents measured along easy (x) and hard (z) axes. (c) Schematic of a uniaxial nanocluster, where H_{al} is the magnetic field used for alignment and γ is the angle between the easy axis and H_{al}. (d) The probability distribution P(γ) of easy axes for Co and Co(Zr) nanoclusters having 7.8 at. % of Zr.

H_c and M_r/M_s are relatively high along the easy axis as compared to those values along the hard axis for Co(Zr) nanoclusters having 6.3 and 7.8 at. % of Zr, revealing a high degree of easy-axis alignment in Co(Zr) nanoclusters by applying a magnetic field prior to deposition. We also estimated the probability distribution of easy axes $P(\gamma)$ of the aligned nanoclusters,[25–28] where γ is the angle between the easy axes and the applied magnetic field H_{al} during the deposition as schematically shown in Fig. 3(c). The Co(Zr) nanoclusters show a narrow $P(\gamma)$ as compared to that of Co nanoclusters.

Co nanoclusters show the following changes of structural and magnetic properties upon Zr addition. First, Co(Zr) nanoclusters show predominant hcp structure, as compared to a mixture of hcp and fcc structures observed in the case of Co nanoclusters. Note that fcc Co has an order of magnitude lower magnetic anisotropy as compared to that of hcp Co and this is supported by significantly enhanced K_1 in Co(Zr) as compared to Co nanoclusters. In conjunction with this result, Co(Zr) nanoclusters show a high degree of alignment by applying a magnetic field prior to deposition.

Note that the actual alignment in the gas phase is a complicated process. The magnetization is rigidly coupled to the crystal in hard-magnetic nanoclusters so that the whole external field (H_{al}) acts on these nanoclusters and aligns them within a few nanoseconds ($H_{\text{eff}} = H_{al} < H_a$), whereas H_{eff} and H_a are effective magnetic field used for the alignment and anisotropy field, respectively. In the case of soft-magnetic nanoclusters such as fcc Co, only the anisotropy field can be exploited ($H_{\text{eff}} = H_a < H_{al}$), and thus the crystal follows with a certain relaxation delay. At the same time, $H_a < H_{al}$ means that thermal excitations are more effective in randomizing the direction between spin and lattice. Qualitative estimates are $MH_{\text{eff}}V/k_BT = 0.5$ for fcc Co and $MH_{\text{eff}}V/k_BT = 5$ for hcp Co, where k_B, V, and T are the Boltzmann constant, volume of the nanoclusters, and temperature, respectively. Furthermore, alignment of the cubic nanoclusters is intrinsically difficult to realize, because interchanging a, b, and c axes does not alter the hysteresis loops.

In summary, a gas-aggregation cluster-deposition system was used to produce dilute $Co_{1-x}Zr_x$ nanoclusters having $0 \leq x \leq 7.8$ and their structural and magnetic properties were investigated. XRD and HRTEM studies show that dilute Co(Zr) nanoclusters have predominantly the hcp structure as compared to a mixture of fcc and hcp phases observed in Co nanoclusters. Co(Zr) nanoclusters also were aligned using a magnetic field of 5 kOe before deposition and the magnetic anisotropy constant was evaluated as a function of Zr content. These results reveal that the addition of Zr to Co nanoclusters improve the magnetic anisotropy and easy-axis alignment process. Co(Zr) nanoclusters having 7.8 at. % of Zr exhibit an appreciable $K_1 \approx 6.8$ Mergs/cm^3 at 300 K as compared to $K_1 \approx 2.1$ Mergs/cm^3 for Co nanoclusters.

This work was supported by the U.S. Department of Energy/BREM (Grant No. DE-AC02-07CH11358, B.D.), Advanced Research Projects Agency-Energy (Grant No. DE-AR 0000046, B.B, G.C.H.), U.S. Department of Energy (Grant No. DE-FG02-04ER46152, D.J.S.), NSF-Materials Research Science and Engineering Center (Grant No. DMR-0820521; R.S. and P.M.), and Nebraska Center for Materials and Nanoscience (X.Z.L.)

[1]D. J. Sellmyer and B. Balamurugan, *Magnetic Technology International* (UKIP Media and Events, Ltd, 2012), p. 41.
[2]N. Jones, Nature **472**, 22 (2011).
[3]A. Pankhurst *et al.*, J. Phys. D: Appl. Phys. **42**, 224001 (2009).
[4]B. Wei *et al.*, Small **2**, 804 (2006).
[5]F. Golkar *et al.*, J. Appl. Phys. **111**, 07B524 (2012).
[6]B. Balamurugan *et al.*, J. Appl. Phys. **111**, 07B532 (2012).
[7]R. Skomski *et al.*, in *REPM'10—Proceedings of the 21st Workshops on Rare-Earth Permanent Magnets and their Applications* (2010), pp. 55–59.
[8]H. Yan and D. E. Laughlin, J. Appl. Phys. **105**, 07A712 (2009).
[9]N. Kikuchi *et al.*, J. Phys.: Condens. Matter **11**, L485 (1999).
[10]B. Balamurugan *et al.*, Appl. Phys. Lett. **101**, 122407 (2012).
[11]H. Haberland *et al.*, J. Vac. Sci. Technol. A **10**, 3266 (2000).
[12]J. M. Qiu, J. Bai, and J. P. Wang, Appl. Phys. Lett. **89**, 222506 (2006).
[13]B. Balasubramanian *et al.*, Nano Lett. **11**, 1747 (2011).
[14]C. Binns *et al.*, Phys. Rev. B **66**, 184413 (2002).
[15]B. Rellinghaus *et al.*, J. Magn. Magn. Mater. **266**, 142 (2003).
[16]B. Balamurugan, D. J. Sellmyer, G. C. Hadjipanayis, and R. Skomski, Scr. Mater. **67**, 542 (2012).
[17]ICCD 2011 International Centre for Diffraction Data, Card No 01-089-4308.
[18]ICCD 2011 International Centre for Diffraction Data, Card No 01-071-4238.
[19]H. Okamoto, J. Phase Equilib. Diffus. **32**, 169 (2011).
[20]G. C. Hadjipanayis, D. J. Sellmyer, and B. Brandt, Phys. Rev. B **23**, 3349 (1981).
[21]A. Franco, Jr. and F. C. E. Silva, Appl. Phys. Lett. **96**, 172505 (2010).
[22]E. Kneller, *Ferromagnetism* (Springer, Berlin, 1962).
[23]D. J. Sellmyer and Z. S. Shan, in *Science and Technology of Nanostructured Magnetic Materials*, edited by G. Hadjipanayis and G. A. Prinz (Plenum Press, New York, 1991), p. 151.
[24]Y. Xu *et al.*, J. Appl. Phys. **97**, 10J320 (2005).
[25]D. L. Roy *et al.*, J. Magn. Mag. Mater. **323**, 127 (2011).
[26]C. Tannous and J. Gieraltwoski, Eur. J. Appl. Phys. **29**, 475 (2008).
[27]D. Givord *et al.*, J. Phys. Colloq. **6**, 46, (1985).
[28]L. Neel *et al.*, J. Appl. Phys. **31**, 27S (1960).